Transactions of the Korean Nuclear Society Spring Meeting
Jeju, Korea, May 9-10, 2024

Analysis of the Dispersion Distance of Molten Salt in Accident Condition

Sung Il Kim*, Hyoung Tae Kim, Hwan Yeol Kim, Rae Joon Park, Eun Hyun Ryu
Intelligent Accident Mitigation Research Division, Korea Atomic Energy Research Institute, (34057) 111, Daedeok-daero 989 beon-gil, Yuseong-gu, Daejeon, Republic of Korea
**Corresponding author: sikim@kaeri.re.kr*

***Keywords :** Molten salt reactor (MSR), safety, explosion, dispersion distance, accident

1. Introduction

Molten salt reactors are gaining global recognition as a promising next-generation energy source for various applications such as ships, mobile units and military, due to their inherent safety features [1-3]. However, depending on the environment in which the molten salt reactor is applied, there may be a need to consider new risk factors that were not previously considered in conventional light water reactor operation. In this study, accident conditions that could occur when utilizing a molten salt reactor system for military purposes were assumed, and the results were analyzed. Given the nature of the military, there is a possibility that the molten salt reactor system could be damaged by enemy shelling. The dispersal of molten salt into the environment in such a scenario provides essential information for establishing operational ranges and strategies for our military thereafter. Therefore, a hypothetical scenario was assumed where the molten salt reactor is directly impacted by enemy artillery fire, resulting in the damage of the reactor vessel. Conservative conditions were assumed, and a preliminary analysis of the maximum dispersal distance was conducted based on the amount of TNT(trinitrotoluene) in the shells.

2. Modeling methods

2.1 Initial volumetric shape modeling of molten salt

As depicted in Figure 1, a cylindrical shape of molten salt with a diameter and height of 1.0 m was assumed. While the actual molten salt reactor vessel reflected in the system may differ slightly in size from those applied in this analysis, updates to the model are planned once the system specifications are finalized. The total number of particles used in this model is 6,320. The presence of the reactor vessel is expected to hinder the dispersal distance of the molten salt during subsequent explosion analysis. Therefore, the reactor vessel's shape serves as a guide for the initial formation of the molten salt volume, disappearing entirely at the moment of explosion to avoid any influence on the analysis. These assumptions were made as part of the effort to derive the maximum dispersal distance [4,5].

2.2 Fluid domain modeling for implementing explosion pressure

Considering the radial direction of explosion pressure and the position of structural elements, the fluid domain for implementing explosion pressure was modeled as a half-sphere shape. In this analysis, to derive the maximum dispersal distance of the molten salt, the location of the TNT explosion was selected where the molten salt could disperse the most. It was assumed that the TNT explodes at the bottom center of the molten salt, as illustrated in Figure 2. In this model, the mass of TNT within the molten salt was configured to be easily modified based on 10, 20, 30, 40, or 50 kg. The size of the fluid domain was assumed to have a diameter of 200 m, as shown in Figure 3.

2.3 Mesh Convergence Study (2D Analysis)

To ensure the reliability of the TNT explosion pressure, a 2D model for mesh convergence was constructed and tested. In this test, incident pressure was evaluated using a fluid-only model, and coupling between particles and fluid flow due to pressure waves was verified. Additionally, tests were conducted to optimize the mesh.

In this test, analysis was conducted to ensure optimal conditions considering explosion pressure, the number and spacing of SPH particles, and analysis time, as shown in Figure 4. Based on this, the size of the fluid domain grid and the characteristics and arrangement of the molten salt particles were determined as follows.

- fluid domain element size (min./max.): 4.5 mm/2.37 m
- distance between particles: 50 mm
- single particle volume: 0.000125 m^3

2.4 Full 3D Particle-Fluid Coupling Analysis

Developed a virtual explosion model incorporating ground effects due to ground detonation conditions. As depicted in Figure 5, differences in explosion pressure behavior depending on the presence of particles were confirmed. Additionally, optimal settings for particle-fluid coupling analysis were obtained.

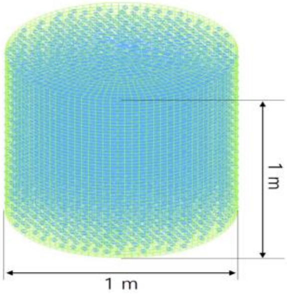

Fig. 1. Finite element and particle model for molten salt.

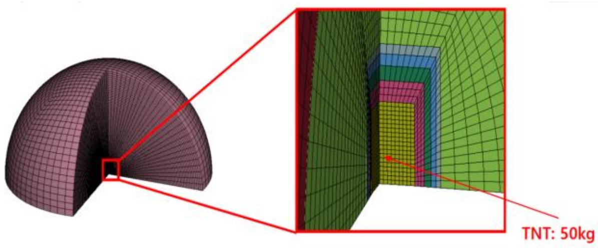

Fig. 2. Fluidic domain and TNT model.

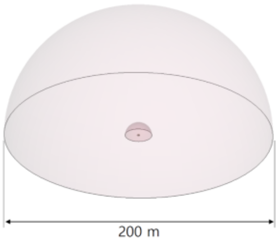

Fig. 3. Fluidic domain geometry.

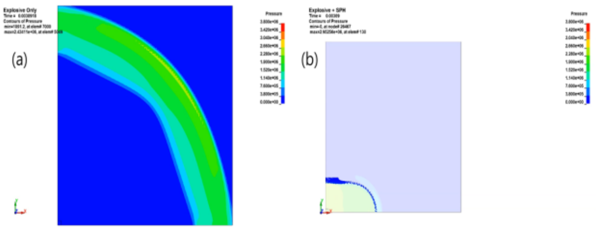

Fig. 4. Mesh convergence analysis(2D): (a) air only, (b) air with particles.

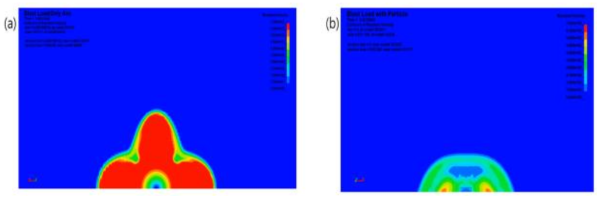

Fig. 5. Velocity distribution due to explosive pressure: (a) air only, (b) air with particles.

2.5 Particle Trajectory Verification Analysis

To verify the prediction formula for the dispersal distance during the free-fall segment, an analysis was conducted. The pressure wave generated by the TNT explosion causes the molten salt particles to disperse, but performing calculations for the dispersal distance over the entire duration using LS-DYNA would take considerable time. Therefore, after the particles disperse and are no longer affected by the pressure wave, they are given initial velocities in three dimensions and evaluated for dispersal distance using the ballistic theory formula, as shown in Figure 6.

For this purpose, a comparison and verification process was carried out by providing three-dimensional initial velocities to the particle-only model and determining the distance when the particles hit the ground, comparing it with the distance obtained through the theoretical formula. Furthermore, it was confirmed that the results of the simulation and calculations based on the theoretical formula exactly matched, as shown in Figure 7.

2.6 Calculation of Dispersal Distance and Post-processing Code Development

From the results of the 3D particle-fluid coupling analysis, the coordinates and velocity information of each particle at the first instance where they are no longer influenced by the explosion pressure (constant velocity segment) can be obtained. At this point, the calculation can be terminated. A code was developed based on the 3D ballistic theory equation to rapidly determine the dispersal distance using the received particle coordinates and velocity information. Additionally, a customized visualization graph code was developed using the calculated dispersal distance.

In the first step, it is verified whether the maximum acceleration of all particles considered in the calculation is less than or equal to the acceleration due to gravity. If all particles satisfy this condition, the calculation is terminated at that point. The criterion for the maximum acceleration of particles is set slightly higher than the acceleration due to gravity at approximately 9.85 m/s^2, aiming to prevent the phenomenon where the acceleration due to gravity of particles remains near 9.81 m/s^2 for a considerable time. By reflecting an error margin of approximately 0.5%, the calculation time was significantly reduced. At the time of termination, the velocity, acceleration, and displacement values of all dispersed particles at each time step were saved.

In the second step, filtering code was developed to input the result values from the LS-DYNA calculation file into our developed code. Specifically, displacement values for each particle over time were derived, and displacement and velocity data for all particles at the last time step were obtained.

In the third step, while calculating displacement (x, y, z) data over time, the x and y values at the point where the height (z) first becomes 0 were utilized as the final dispersal distance result. A program was developed to output the calculated x and y values for each particle on a visualization graph. The visualized dispersal distance distribution results obtained through the program are as shown in Figure 8. This program presents dispersal

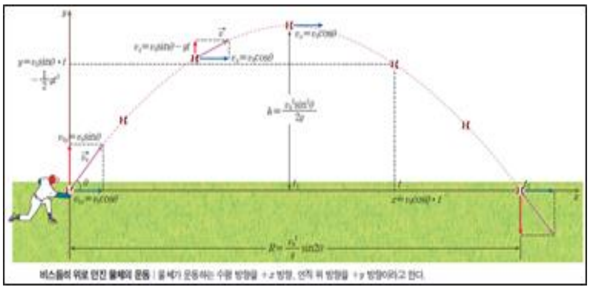

Fig. 6. Projectile motion formula in 2D plane.

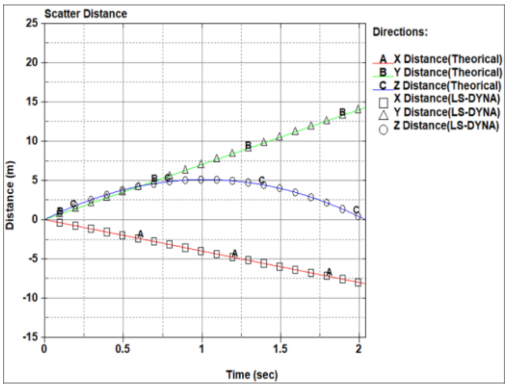

Fig. 7. Analysis result comparison with program calculation.

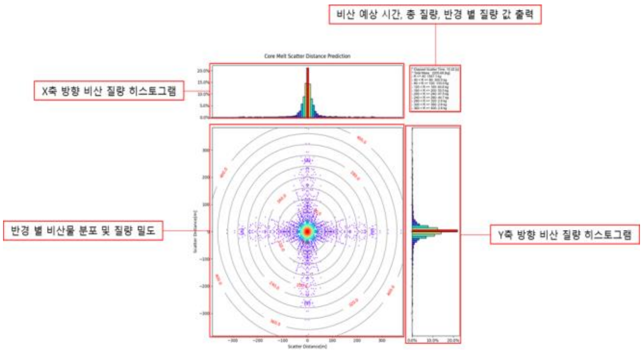

Fig. 8. Visualization of dispersal distance results.

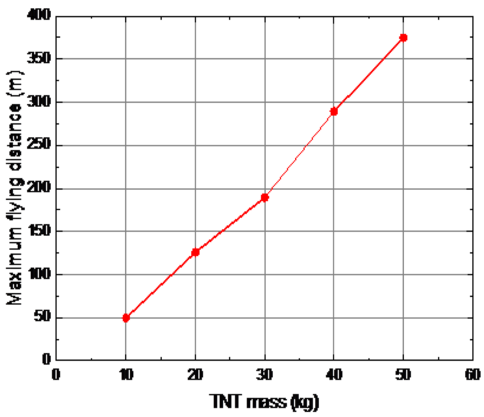

Fig. 9. Maximum dispersal distance with TNT mass

mass histograms in the x and y directions, along with dispersal material distribution and mass density by radius, estimated dispersal time, total mass, and mass values by radius [6-8].

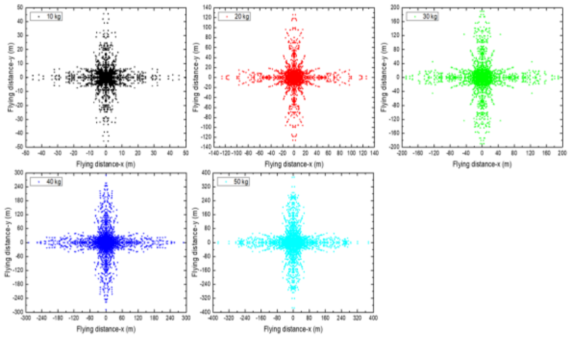

Fig. 10. SPH particle distribution with TNT mass (1).

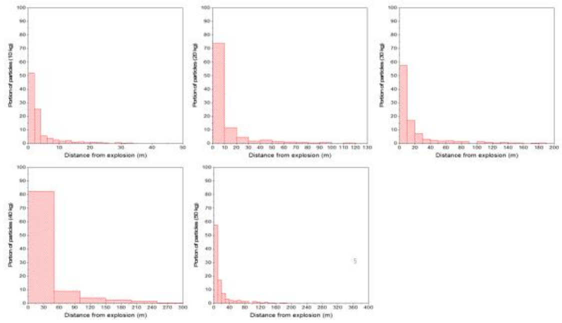

Fig. 11. SPH particle distribution with TNT mass (2).

3. Results

We performed calculations by incrementally increasing the TNT mass from 10 kg to 50 kg with increments of 10 kg and obtained the results. The molten salt properties considered in this ana

lysis are NaCl-$MgCl_2$-$TRUCl_3$. In the future, if the molten salt composition changes, the input properties can be adjusted accordingly for calculations.

The maximum dispersal distances according to the TNT mass are presented in Figure 9. As the TNT mass increases from 10 kg to 50 kg in increments of 10 kg, the maximum dispersal distances show a linear increase, being 49.6 m, 125.8 m, 189.5 m, 289.4 m, and 374.7 m, respectively.

The dispersal distance distribution of molten salt particles according to the TNT mass is shown in Figure 10. Overall, a similar dispersal pattern was observed. The directional dispersal is attributed to two main factors: the cubic shape of the TNT model, causing the mass to be slightly more distributed in four directions, and the ground effect, where pressure waves reflected from the ground overlap with those generated during the explosion, resulting in directional effects. Further analysis of these causes will be conducted in the future.

The dispersal distance distribution of molten salt according to the TNT mass is presented in Figure 11. The analysis results show that approximately 90% of the dispersed particles are located within approximately 25% of the maximum dispersal distance in all cases. This indicates that most dispersed particles do not travel significantly far from the explosion point and remain relatively close to it.

4. Conclusions

In this study, we quantitatively evaluated the dispersal distance of molten salt inside the transportable molten salt reactor system when it is damaged by external attacks such as shelling. To achieve this, we proposed a model for evaluating the dispersal distance and established a methodology through assumptions. Liquid molten salt was assumed to be represented by SPH particles for analysis, and calculations were conducted under the most conservative conditions to obtain the most cautious results.

Through this study, we developed an input model for evaluating dispersal distance and preliminarily assessed the maximum dispersal distance and distribution of molten salt according to the TNT mass. We calculated and analyzed the dispersal distance as the TNT mass increased in increments of 10 kg from 10 kg to 50 kg. It is presented the distance at which molten salt could disperse maximally, and it was confirmed that most of the molten salt did not travel significantly far from the explosion point. These analysis results serve as preliminary assessments, and continuous model improvement work is planned.

ACKNOWLEDGEMENT

This work was supported by Korea Research Institute for defense Technology planning and advancement(KRIT) grant funded by the Korea government(DAPA(Defense Acquisition Program Administration)) (KRIT-CT-22-017, Next Generation Multi-Purpose High Power Generation Technology(Liquid Fuel Heat Generator Transportation and Safety Assessment Technology), 2022)

REFERENCES

[1] David E. Holcomb, Alexander J. Huning, Randall J. Belles, George F. Flanagan, Willis P. Poore, Integrating the Safety Evaluation for a Molten Salt Reactor Operation and Fuel Cycle Facility Application, ORNL/TM-2022/2671.
[2] U.S.NRC, SCALE/MELCOR Non-LWR Source Term Demonstration Project –Molten Salt Reactor (MSR), SAND2022-12146 PE, September 13, 2022.
[3] Sara Thomas and Josh Jackson, MSR Salt Spill Accident Testing Using Eutectic NaCl-UCl3, ANL/CFCT-22/32.
[4] Yakov I. Rabinovich, Madhavan S. Esayanur, and Brij M. Moudgil, Capillary Forces between Two Sphrees with a Fixed Volume Liquid Bridge: Theory and Experiment, Langmuir 2005, 21, 10992-10997.
[5] John S. Peake and Marvin R. Bothwell, The Surface Tensions and their Temperature Coefficients of Molten Mixtures of Potassium Chloride and Barium Chloride, 1954, J. Am. Chem. Soc. 76, 10, 2656-2659.
[6] LIVERMORE SOFTWARE TECHNOLOGY (LST), AN ANSYS COMPANY, LS-DYNA KEYWORD USER'S MANUAL VOLUME I, 2021.
[7] LIVERMORE SOFTWARE TECHNOLOGY (LST), AN ANSYS COMPANY, LS-DYNA KEYWORD USER'S MANUAL VOLUME II Material Models, 2021.
[8] LIVERMORE SOFTWARE TECHNOLOGY (LST), AN ANSYS COMPANY, LS-DYNA KEYWORD USER'S MANUAL VOLUME III Multi-Physics Solvers, 2021.